PALEOCEANOGRAPHY, VOL. 106, XXXX, DOI:10.1029/2001JA900021, MAR 2006

ENSO as a mediator for the solar influence on climate

Julien Emile-Geay, Mark Cane, Richard Seager, Alexey Kaplan, and Peter Almasi

Lamont-Doherty Earth Observatory of Columbia Unversity, Palisades, New York

---

Julien Emile-Geay, Lamont-Doherty Earth Observatory of Columbia University, Oceanography 301F, 61 Route 9 W, Palisades, NY 10964-8000. e-mail: julieneg@ldeo.columbia.edu

Abstract. Using a climate model of intermediate complexity, we simulate the response of the El Niño -Southern Oscillation (ENSO) system to solar and orbital forcing over the Holocene. Solar forcing is reconstructed from radiocarbon production rate data [*Bond et al.*, 2001], using various scaling factors to account for the conflicting estimates of solar irradiance variability [*Fröhlich and Lean*, 2004]. As estimates of the difference since the Maunder Minimum range from 0.05 % to 0.5 % of the solar "constant" , we consider these two extreme scenarios, along with the intermediate case of 0.2%, corresponding to differences of, respectively, 0.17, 0.68 and 1.7 Wm^{-2}, in terms of top-of-the-atmosphere insolation. We show that for large or moderate forcings, the low-passed filtered east-west sea-surface temperature gradient along the equator responds linearly to irradiance forcing, with a phase lag of less than a year. In contrast, the 0.05%-case shows no significant variability above that inherent to the model's chaotic behavior. Wavelet analysis suggests a statistically-significant enhancement of the century-to-millenial scale ENSO variability for moderate-to-strong irradiance forcing. Orbitally-driven insolation forcing is found to produce a long-term trend of increased ENSO variability from the early Holocene onwards. It adds approximately linearly to the solar response. Given the importance of ENSO in the climate system, the results suggest a potentially significant mechanism for long-term solar irradiance variability as a driver of natural climate change. A comparison to key Holocene climate records, from the Northern Hemisphere subtropics and midlatitudes, show support for this hypothesis.

1. Introduction

The concept of a solar influence on the Earth's climate is hardly new. Sunspots were a favored explanation for monsoon failures as early as 1875 [see *Davis*, 2001, ch 7], and the link between the Maunder Minimum and the Little Ice Age was made a century later [*Eddy*, 1977] (for a recent review, see *Rind* [2002]). Since solar radiation is the primary source of energy driving atmospheric and oceanic flow, and since its intensity is thought to vary on long timescales (see *Fröhlich and Lean* [2004] for a review), it is often invoked to explain natural climate change on decadal [*van Loon and Labitzke*, 1988] to multicentennial timescales [e.g. *Jones and Mann*, 2004]. The puzzling fact is that even generous reconstructions of past total irradiance changes do not yield changes bigger than $1.7\ \mathrm{W m^{-2}}$. The challenge is to understand how these subtle radiative fluctuations could emerge as a significant driving force of the Earth's climate, a system showing a considerable degree of internal variability.

In a seminal paper, *Bond et al.* [2001] demonstrated an intriguing correlation between proxies of solar activity and the quantity of ice-rafted debris in the North Atlantic, and concluded there was a "persistent solar influence on climate" during the Holocene. Recent years have seen the accumulation of an impressive body of geological evidence indicating that the Sun's activity has varied on centennial to millennial timescales [*Stuiver et al.*, 1991; *Bard et al.*, 2000; *Beer*, 2000]. This information is obtained from the atmospheric concentration of cosmogenic isotopes (primarily $^{10}\mathrm{Be}$ and $^{14}\mathrm{C}$) as recorded in tree-rings and ice cores. The reasoning goes as follows : since the open magnetic flux of the Sun is more intense during periods of increased irradiance, and since it deflects the cosmic rays producing the isotopes in the Earth's upper atmosphere, then the fluctuations in the atmospheric isotopic concentrations must be anticorrelated with the Sun's

radiative output. Using various corrections for the geomagnetic shielding and the geochemical cycling of cosmogenic isotopes, one can theoretically isolate the effect of solar activity in ice core $^{10}\mathrm{Be}$ and tree-ring $^{14}\mathrm{C}$. The method is not devoid of problems (see, for instance *Marchal* [2005] and *Saint-Onge et al.* [2003]), and to begin with, the positive correlation between the indirectly recorded solar open magnetic flux and total solar irradiance - let alone the dynamical mechanism - is not firmly established [*Lean et al.*, 2002; *Foukal et al.*, 2004].

Prompted by Bond's work, however, a number of investigators have attempted to understand this link. So far, the main dynamical pathway from the Sun to the surface has invoked the stratosphere and its effect on planetary wave propagation [e.g. *Geller and Alpert*, 1980; *Haigh*, 1996]. Fluctuations in the ultra-violet (UV) spectral band have been shown to alter stratospheric ozone photochemistry, and therefore latitudinal temperature gradients in the lower stratosphere. This translates into changes in the index of refraction of upward-propagating planetary waves, which forces a redistribution of momentum fluxes throughout the troposphere, eventually leading to surface climate change, mainly over northern hemisphere continents [*Shindell et al.*, 1999]. More recent accounts describe a mechanism with a very different premise, but with similar route through the stratosphere : *Shindell et al.* [2001] propose that, with increased irradiance, "*(i) tropical and subtropical SSTs warm, leading to (ii) a warmer tropical and subtropical upper troposphere via moist convective processes. This results in (iii) an increased latitudinal temperature gradient at around 100 to 200 mbar, because these pressures are in the stratosphere at higher latitudes, and so do not feel the surface warming. The temperature gradient leads to (iv) enhanced lower stratospheric westerly winds, which (v) refract upward-propagating tropospheric planetary waves equatorward. This causes (vi) increased angular momentum transport*

to high latitudes and enhanced tropospheric westerlies, and the associated temperature and pressure changes corresponding to a high AO/NAO index."

In this paper we explore a different pathway of solar influence on climate, one centered around the El Niño -Southern Oscillation (ENSO) (that is to say, of purely tropical origin), and irrespective of the spectral signature of solar changes. Following *Mann et al.* [2005] and *Clement et al.* [1999], we employ the Zebiak-Cane model [*Zebiak and Cane*, 1987] and diagnose its reaction to solar and orbital forcing over the past 10,000 years, in a variety of experiments. We show that even in the face of realistic amounts of weather noise, low-frequency solar irradiance fluctuations induce non-negligible changes in the east-west temperature gradient, and in ENSO activity. The magnitude of the changes, albeit subtle, is enough to produce sizable impacts on the extratropical hydrological cycle around the Pacific [*Seager et al.*, 2005b]. A surprising result which will be explained is that, weak though it is, solar irradiance fluctuations produce SST changes of the same magnitude as those produced by precessional forcing, though the latter forcing is greater by at least an order of magnitude. It can also generate sizable impacts over the globe, in particular over the North Atlantic, with a noticeable hemispherically-symmetric component [*Seager et al.*, 2003] - as opposed to the planetary wave mechanisms described above.

The paper is structured as follows : in section 2 we describe the climate forcings at work during the Holocene. In section 3 we describe the experimental setting, before presenting the results (section 4), whose global implications are analyzed in section 5. Discussion follows in section 6.

2. Climate forcing over the Holocene

Given our model's formulation in terms of anomalies (see section 3), the climate forcings of interest are departures from the current radiative budget, which gave rise to the late twentieth century climatology embedded in the model. One has to first consider fluctuations in solar forcing arising from the changes in the Earth's orbit ("orbital forcing"), as in *Clement et al.* [1999]. Second, one must consider changes in the actual solar irradiance ("solar forcing"). We briefly discuss other potentially important forcings.

2.1. Orbital forcing

The orbital forcing is the best-known piece of the puzzle, and can be readily and accurately computed [*Berger*, 1978]. Here we characterize its effects via an empirical orthogonal function (EOF) analysis of the insolation in the (calendar month, latitude) state space, with time marching annually for the past million years. The latitude grid is restricted to the band [29°S; 29°N] - the model domain.

In Fig 1 we show the first 3 EOFs, accounting for 99.7% of the variance over the Holocene. The first two EOFs are clearly associated with precession, with a peak at a period of 23 kiloyear (ky), zero annual mean and weak dependence on latitude. EOF1 is associated with the summertime/wintertime insolation contrast near the equator. Similarly, EOF2 can be described as the spring-fall insolation contrast at the equator. Although the two PCs are, by definition, orthogonal over the last million years, they are significantly correlated ($\rho \sim 0.5$) over the Holocene. The third EOF is associated with obliquity changes, with a period of 43 ky, and the two hemispheres are out-of-phase. It is only of minor importance for the Holocene in the tropics (it only accounts for 0.84% of the variance). Overall, these three EOFs fully describe the orbital forcing

of relevance for tropical climate. In particular, they show that the northern hemisphere summer-winter contrast has kept decreasing since the early Holocene, and so has the fall-spring contrast, since about 5000 B.P.

2.2. Solar irradiance forcing

As emphasized in the Introduction, reconstructions of past solar irradiance variations are a matter of considerable debate and vexingly large uncertainties. The reconstructions rely on sunspot observations for recent centuries, and on paleoproxy records of cosmogenic nuclides for the longer record. The latter are directly influenced by changes in magnetic flux from the Sun, not changes in irradiance. A relationship between the two must be created by extrapolating from the short period of instrumental observations, inferring a low-frequency irradiance component from observations of the group sunspot number gathered since the invention of the telescope (see *Fröhlich and Lean* [2004] and references therein). There is no obvious way to perform this extrapolation.

As a proxy for solar activity, we use the $^{14}\mathrm{C}$ production rate ($\mathcal{P}^{14}\mathrm{C}$), in the spectral range where it most resembles $^{10}\mathrm{Be}$, so that confidence can be gained that both nuclides were recording solar activity. Indeed, Be and C have such different geochemical cycles that their coherent behavior must reflect a common source : the Sun's magnetic activity. Smoothing the tree-ring $^{14}\mathrm{C}$ production rate (from INTCAL98, *Stuiver et al.* [1998]) and ice core $^{10}\mathrm{Be}$ record [*Yiou et al.*, 1997] to isolate periods longer than ~ 500 years, *Bond et al.* [2001] found they were highly coherent (0.93) in the 900 to 1100-year band. We therefore take this smoothed $\mathcal{P}^{14}\mathrm{C}$ record as our proxy of solar activity.

In doing so, we note that the documented Gleissberg (~ 88 yr) and DeVries (~ 205 yr) cycles [*Peristykh and Damon*, 2003; *Wagner et al.*, 2001] are suppressed. Hence, centennial variability is probably underestimated in the forcing - and as we shall see, in the response. However, as $\mathcal{P}^{14}\mathrm{C}$ does not seem to covary with the $^{10}\mathrm{Be}$ record in those spectral bands , we take a more conservative stance and prefer not to include them.

There remains the problem of translating the loosely defined "solar activity" into irradiance. Though sophisticated techniques have been applied to this end [*Mordvinov et al.*, 2004], no such reconstruction is available for the Holocene at the time of publication. We therefore apply the linear scaling of *Bard et al.* [2000] : the reference scale (ΔF) here is the difference in TSI/4 (total solar irradiance, divided by 4 because of spherical geometry) from the Maunder Minimum (roughly 1645 to 1715 A.D.) to the "present" (1950 A.D.). It is essentially the sunspot number difference multiplied by the slope of the scatterplot of irradiance versus sunspot number. The latter, as discussed above, is only based on about 20 years of reliable radiometric data. Since published estimates of the difference [*Foukal et al.*, 2004; *Fröhlich and Lean*, 2004] range from $\Delta F = 0.05\%$ to 0.5 % of the solar "constant" ($S_\circ = 1366\ \mathrm{W m^{-2}}$ for consistency with *Berger* [1978]), we consider these two extreme cases, along with the intermediate case of 0.2%, corresponding to peak-to-peak differences of, respectively, 0.17, 0.68 and 1.7 $\mathrm{W m^{-2}}$. The 0.2% case is close to the value used by *Crowley* [2000] and *Weber et al.* [2004]. It is worth emphasizing that most recent estimates are on the lower end of this interval [*Foukal et al.*, 2004; *Fröhlich and Lean*, 2004], though the solar physics community is far from having reached a consensus on the issue. Also, these long-term changes are thought to have a marked maximum in the

UV domain, but recent GCM experiments show that the atmosphere's response is somewhat indifferent to the spectral signature of the forcing [*Rind et al.*, 2004].

In Fig (2) we show the 3 scalings of the solar forcing and a spectral analysis of the smoothed $\mathcal{P}^{14}\mathrm{C}$ timeseries. We use singular spectrum analysis (SSA) [*Vautard and Ghil*, 1989; *Ghil et al.*, 2002] to enhance the signal-to-noise ratio of the index and compute the spectrum using the multi-taper method (MTM) [*Thomson*, 1982], which show the prominence of millennial-scale variability. A wavelet spectral density and global wavelet spectrum, computed by the method of *Torrence and Compo* [1998], confirm the presence of peaks within the millennial band isolated by the filtering of *Bond et al.* [2001] and hints to a bi-millennial one in the first half of the Holocene, but the MTM spectrum suggests that it is below the level of a theoretical AR(1) process.

2.3. Volcanic forcing : a Holocene record is still needed

Mann et al. [2005] have conducted very similar experiments with the same model, forced by solar and volcanic radiative perturbations over the past millennium. They found that volcanic forcing (of order 1 to 10 $\mathrm{W m^{-2}}$) generally produces a much greater response than solar forcing and, for the stronger eruptions, consistently produces El Niño events in the model. However, they also found that the persistent nature of solar irradiance forcing confers it an important role in governing low-frequency ENSO variability. Clearly then, a complete analysis of Holocene climate forcings should include an estimate of sulfate aerosol loading in the lower stratosphere, but a dataset of such length is currently unavailable. The present study is limited to an examination of solar and orbital forcing of ENSO. A more complete analysis of Holocene ENSO will require accounting for Tropical volcanic forcing if and when such data becomes available.

3. Experimental Setting

3.1. The model

We use the model of *Zebiak and Cane* [1987]. It is a model with linear shallow-water dynamics for the global atmosphere [*Gill*, 1980; *Zebiak*, 1982] and the Tropical Pacific ocean [*Cane and Patton*, 1984], coupled by non-linear thernodynamics, which give the model self-sustained ENSO variability. The ocean model domain is restricted to [124°E- 80°W; 29°S- 29°N], which means that only tropical processes are considered. The model is linearized around a constant climatology [*Rasmussen and Carpenter*, 1982].

We employ the same configuration as *Clement et al.* [1999], in the model version written by Takashi Kagimoto at the International Research Institute for Climate Prediction. Radiative forcing anomalies are included as a source term of the (prognostic) equation for sea-surface temperature (SST). Conversion is made from the top-of-the-atmosphere pertubation to a surface flux by multiplying by $(1 - 0.62\ \mathrm{C} + 0.0019\alpha)$ where C is the cloud fraction and α is the noon solar altitude [*Reed*, 1977]. Consistent with the absence of radiative scheme in the model, we hold the cloud fraction constant, 50%. As in *Mann et al.* [2005], the solar forcing estimates are multiplied by a factor of $\pi/2$, since the model represents only the Tropics.

3.2. Representation of Weather Noise

It is well known that the tropical Pacific ocean-atmosphere system is the stage of considerable interannual and intraseasonal variability. Whether one is the child of the other is a question beyond the scope of this paper. Whether ENSO, in nature, is self-sustained or stochastically-forced, the question relevant to the present study is whether the ENSO system would notice solar irradiance perturbations in the presence of a physically realistic amount of weather noise.

The latter concept encompasses all wind fluctuations that are external to the coupled subsystem, which our model is designed to represent. The simplest way to parameterize this phenomenon is to characterize it by a uniform patch of westerlies over the western equatorial Pacific (hereafter WP, spanning [165°E- 195°E, 5°S- 5°N]). Its amplitude is the fraction of monthly windstress variability that is not accounted for by a direct response to SST forcing. To represent this, we choose a statistical model that crudely approximates the low-order moments of the observed τ_x. An autorregressive model of order 1 [AR(1)] seems appropriate for such a process. Its time-integrated variance ${\sigma_N}^2$ is set to a fixed value via the relation $\sigma_N = \ell\, \sigma_{\mathrm{NCEP}}$. Multi-member ensemble experiments with a state-of-the-art coupled ocean-atmosphere general circulation model (OAGCM) suggest that about 15% to 20% of the WP montly-mean wind variance is unrelated to SST, and can therefore be described as weather noise (A.Wittenberg, personal communication). We choose a noise *level* of $\ell = 40\%$ as our canonical value, corresponding to a noise *variance* of 16% of the total. The AR(1) parameter is the lag-1 autocorrelation of monthly τ_x over the WP, estimated from NCEP data at $\alpha = 0.73$.

The AR(1) processes $X(t)$ are generated numerically, and the wind noise $\tau_x^N(t) = \ell\, X(t)$ is then applied uniformly onto the WP box for the whole length of the simulation.

We summarize in Table 1 the different numerical experiments conducted in this study.

4. Results

4.1. Solar

In the following, we focus on the ensemble-mean zonal SST gradient along the equator (EW), which is the difference between the WP index (average SST over the aforementioned western

Pacific box) and the NINO3 index (average SST over [150°E- 90°W, 5°S- 5°N]). This procedure removes any zonally-uniform temperature change and reduces the noise significantly.

In Fig 3 we present the results of the model forced by reconstructed solar irradiance ($\Delta F = 0.5\% S_o$), in a 6-member ensemble. As is apparent from panel (a), the 40-year low-passed EW responds almost linearly to the irradiance forcing, with an amplitude of 0.3 °C. While this may look insignificant at first sight, recent research on the origin of North American drought has convincingly demonstrated, using two different general circulation models, that La Niña anomalies of such amplitude generated the sequence of severe droughts that visited the American West since the mid-nineteenth century, including the 1930s [*Schubert et al.*, 2004; *Seager et al.*, 2005b; *Herweijer et al.*, 2006a]. SST variations this small, if persistent enough, are sufficient to alter extratropical atmospheric circulation and perturb local hydroclimates in the Western US, South America, and elsewhere [*Herweijer and Seager*, 2006].

Panel (b) shows the wavelet spectral density [*Torrence and Compo*, 1998] of the same EW index, obtained with the Morlet mother wavelet with 6 scales per octave. Though non-stationary, the signal generally shows the highest power in the ENSO band (2 to 7 yr period, centered around 4 yr) and the millennial band ($\sim$ 500 to 2000 yr) where the solar forcing displays its maximum variance. However, variability in this band could be entirely due to the model's internal chaotic dynamics, as shown by *Clement et al.* [1999]. We therefore devise the following test : from a 150,000 year long unforced run of the model, we extract 400 timeseries of the same length as the simulations of interest (i.e. 12060 years), with starting times picked at random more than 100 years apart. We perform the wavelet analysis on each of those timeseries,

compute their global wavelet spectrum and for each scale, sort the spectra in increasing order. The upper 20 thus define the 95% confidence level.

From this we can see on panel (c) that only in the millennial band does the model response exceed its level of natural variability at the 95% level. Interestingly, the model internal variability does exhibit a weak peak in this band, though it knows of no numerical constant or physical process that could have introduced such a timescale. It is an illustration that the nonlinear atmosphere/ocean feedbacks it embodies can generate variability at unexpectedly long periods. The fact that it also responds to forcing at such frequencies could be perceived as a form of damped resonance, but this is not the case : perturbing the model by a white-noise radiative forcing with the same variance as the $\Delta F = 0.2\% S_o$ case, we find that variability is raised uniformly at all frequencies, and that the millennial scale is not favored.

Note that this approach implicitly assumes that the timeseries extracted from the unforced run are statistically independent, which may seem contradictory, as they are part of the same realization of a numerical dynamical system. We assert that independence is true for all practical purposes, as predictability studies with the same model [e.g. *Karspeck et al.*, 2004] show that its NINO3 index is of very limited predictability even a decade or two in advance.

Why does the model respond with increased SST gradient to positive radiative forcing ? This may be understood as follows [*Clement et al.*, 1996] : if there is heating over the entire tropics, then the Pacific will warm more in the west than in the east because the strong upwelling and surface divergence in the east moves some of the heat poleward. Hence the east-west temperature gradient will strengthen, causing easterly winds to intensify, further enhancing the zonal temperature gradient (the *Bjerknes* [1969] feedback). This process leads to a more La

Niña-like state (positive values of the EW index) in response to increased irradiance. Such an adjustment typically occurs over a few years to a decade, so that on millennial timescales, it looks virtually instantaneous. The dynamical feedback that makes the SST harder to change in the east has earned the name "thermostat" to this mechanism.

Finally, we present in panel (d) the probability of a strong El Niño event (NINO3 > 2 K for a year) on a 200-year window amongst all six ensemble members, as a measure of ENSO variability *per se*. The index does show centennial to millennial cycles, but no obvious trend, unlike the orbitally-forced model, as we shall see.

4.2. Orbital

In Fig 4 we show the same quantities as before, in the case of the orbitally-forced run. High wavelet spectral density is expected at orbital timescales, but its exact value is unreliable in this calculation, as it mostly lies within the "cone of influence" [*Torrence and Compo*, 1998]. Notice the small centennial-to-millennial power in this case, in contrast to the solar case.

The salient feature is the growing intensity of ENSO activity from the mid-Holocene onwards, which can be seen either in the wavelet spectrum (b) or the probability of large ENSO events (d). The latter features a prominent upward trend, with the probability of a strong El Niño doubling between 10,000 years BP and 800 BP (from 0.09 to 0.18). A similar finding was noted by *Clement et al.* [2000] and qualitatively supported by a flood proxy from Lake Pallcacocha [*Moy et al.*, 2002] and high-resolution coral δ^{18}O from the Huon Peninsula [*Tudhope et al.*, 2001].

The dynamical explanation for why ENSO has a low variance at times of stronger seasonality is given by *Clement et al.* [1999]. The reason is that the seasonal migration of the inter-tropical convergence zone (ITCZ) modulates the effective coupling strength [*Zebiak and Cane*, 1987],

so that the system is most responsive to radiative anomalies centered around July : an increased insolation at that time of the year is then translated as a cooling in the eastern equatorial Pacific via the "thermostat" mechanism described above. This tends to suppress the growth of large El Niño events at times where the summertime insolation was much stronger than now - such as the early Holocene. As this seasonal contrast wanes over the course of the Holocene, ENSO variance steadily grows towards modern-day values.

4.3. Orbital & Solar

We now consider the model response when solar and orbital forcing act together. In this we neglect the interaction between solar and orbital forcing anomalies, i.e. the anomalous orbital motion working on the anomalous irradiance, since the product is found too small to be of significance.

The model response is presented in Fig 5, with the same conventions as before. Notice that the wavelet spectral density in the millennial band is virtually identical to that of Fig 3 (solar forcing alone), with the added low-frequency component at orbital timescales (> 8000 years).

It is noteworthy that although solar forcing has peak-to-peak variations of $\sim 2\ \mathrm{Wm}^{-2}$, compared to a summer-winter insolation difference peaking at $\sim 40\ \mathrm{Wm}^{-2}$, their effect is disproportionately large : EW temperature responses are of similar amplitude for the two forcings. Though we have emphazised that the system is most poised to radiative pertubations in late summer/early fall, the fact that solar forcing has a non-zero annual mean signal - unlike precessional forcing, which dominates the orbital part - plays an important role in the model.

How much of the ENSO variability can be linearly predicted from knowledge of solar irradiance and the Earth's orbital parameters ? We consider the 18 realizations of the model forced by

orbital and moderate solar forcing ($\Delta F = 0.2\%$), and perform a multivariate regression of the smoothed, ensemble-mean EW timeseries over three variables : PC_1 and PC_2 from the EOF analysis presented in Fig(1) and the solar irradiance F_o from Fig 2. EW was lowpass-flitered at periods longer than 200 years with a Gaussian window prior to normalization.

The result is shown in Fig 6 : the upper panel presents the dependent variable and its predictors ; the lower panel shows the result of the regression.

The linear correlation coefficient between predicted and "observed" timeseries is very high ($\rho \simeq 0.85$). Such a correlation means that about 72% of the timeseries variance can be explained by the linear response to the forcing, with orbital forcing accounting for about 41% and irradiance fluctuations for 31%. This ratio does not change qualitatively over a wide range of cutoff frequencies, though, as expected, the higher the cutoff, the lesser the fraction of variance explained by the millennial-scale forcing. Thus, with a 40-year lowpass as on Fig 3, 4, or 5, the total variance explained by the forcing is only 45%, with 26% of orbital origin and 19% of solar origin.

We conclude that solar perturbations of mid-range amplitude are sufficient to generate persistent SST anomalies of a fraction of a degree on millennial timescales, via the thermostat mechanism. We find supporting evidence for this in records of the past millennium. *Mann et al.* [2005] show that their result is consistent with the Palmyra ENSO record of *Cobb et al.* [2003] : at times of increased irradiance, such as the Medieval Warm Period (900-1300 AD), the average conditions were colder in the eastern equatorial Pacific (La Niña-like). Conversely, they were warmer (El Niño-like) during the Little Ice Age (1600-1850 AD), when solar irradiance was weaker.

Irradiance fluctuations also prove comparatively efficient at altering ENSO statistics, even in the presence of the much greater orbital forcing. Hence, ENSO may have acted as a recipient and transmitter of solar influence. The question is now : did such changes spread to other latitudes, and is the global paleoclimate record consistent with them ?

5. Global implications

5.1. Solar-induced ENSO and North America

North America is one of the regions of the world with the strongest teleconnection pattern to the tropical Pacific. The same drought patterns linked to tropical Pacific SSTs in the instrumental period are also found in tree-ring reconstructions of Palmer Drought Severity Index from the North American Drought Atlas for the medieval climate anomaly and Little Ice Age [*Cook et al.*, 2004, 2006]. This adds further credence to the theory. *Herweijer et al.* [2006b] review additional evidence for a La Niña-like global hydroclimate during the medieval climate anomaly.

Recent data by *Asmerom et al.* [2005] support the notion of an anticorrelation between solar activity (tree-ring $\Delta^{14}\mathrm{C}$) and oxygen isotopic composition of uranium-series dated speleothems in the American Southwest, taken as a proxy for ENSO-related precipitation over the entire course of the Holocene. Given that the model only predicts the ensemble *average* SST gradient to closely follow the forcing, we would not expect the one realization provided by nature to match it exactly. On the contrary, the observed correspondence is in fact remarkable.

5.2. Solar-induced ENSO and the North Atlantic

We now go back to the original observation that motivated this work, and ask whether this theory can explain the IRD record of *Bond et al.* [2001].

The idea that Indo-Pacific SSTs can alter the climate of the North Atlantic was recently advanced by *Hoerling et al.* [2001], who used an atmospheric general circulation model (GCM) forced by historical SSTs in various basins (namely, the whole globe (GOGA) or solely the Tropics (TOGA)). They attributed the late twentieth century upward trend of the North Atlantic Oscillation (NAO) to the SST warming trend of the western equatorial Pacific and Indian Oceans, most likely due to anthropogenic greenhouse forcing. Accordingly, increased solar irradiance and a reduced SST gradient would be expected to push the NAO into a more positive phase. A problem with this view is that one has, thus far, been hard-pressed to find evidence of stable correlations in the entire instrumental record [*Rogers*, 1984], or even in other GCM experiments.

The likely source of hematite-stained grains (HSG) found in the cores of the Denmark Strait and west of Ireland (VM28-14 and VM29-191) is in the Arctic or the Nordic Seas [*Bond et al.*, 2001]. It also seems likely that the debris were rafted by sea-ice rather than icebergs (Bond, 2005, personal communication). *Bond et al.* [2001] argued that two ingredients were necessary to explain the synchronous increase in IRD tracer percentages at these and other coring sites distributed across the subpolar North Atlantic during Holocene millennnial events :

1. a basin-wide cooling necessary for the ice to survive at such latitudes

2. northerly winds over key regions such as the Denmark and/or Fram straights (necessary for the southward sea-ice advection), at least during part of the year.

Therefore, we seek evidence of northerly winds in association with El Niño-like states of the tropical Pacific. We use wind field data from three sources :

- **the GDFL coupled model** (version 2.1) simulation H1

(http://nomads.gfdl.noaa.gov/CM2.X/CM2.1/data/cm2.1_data.html). The forcing for this simulation is a reconstruction of natural and anthropogenic radiative perturbations over the period 1860-2000. This simulation has a vigorous, self-sustained ENSO with variance comparable to that observed. Very similar results were obtained with simulations H2 and H3.

• **POGA-ML simulations with the NCAR CCM3 model**, as used in *Seager et al.* [2005b]. The AGCM is coupled to a two-layer, entraining, mixed-layer ocean model, with SSTs prescribed only in the tropical Pacific (computed elsewhere). The results analyzed are the average of a 16-member ensemble, which isolates the influence of the boundary conditions - in this case, tropical Pacific SSTs over the period 1860-2000. The data can be found at http://kage.ldeo.columbia.edu:81/expert/SOURCES/.LDEO/.ClimateGroup/.MODELS/.CCM3/.PROJECTS/.poga-ML/.poga-ML-mean/. In both models we analyzed the wind *stress*, since it is the most relevant to surface ocean dynamics.

• **Our best observational estimate** of surface winds over the North Atlantic. Stress estimates were unfortunately unavailable before 1949, so the wind *velocit*y field was taken from the analysis of *Evans and Kaplan* [2004], which uses an optimal interpolation (OI) of ICOADS winds (http://icoads.noaa.gov/, [*Worley et al.*, 2005]). This has the effect of retaining the large-scale features of the field, which are most relevant for our study.

The period of analysis was the longest common to all datasets, 1860-2000. All fields were smoothed by a 3-month running average. They were then regressed onto the corresponding NINO3 index : in the last two examples, the latter was computed from the extended SST analysis

of *Kaplan et al.* [1998], while the model-generated NINO3 index was used in the first example (GFDL H1).

Results are shown in Fig 7 : the left-hand panels show the covariance of surface wind-stress (or velocity when analyses of stress were not available) with NINO3, and the right-hand ones show the linear correlation maps of the meridional wind component. All datasets are in broad agreement that northeasterly winds tend to occur over the area of interest during periods of high NINO3. Nonetheless, the amplitudes are weak and it is necessary to establish whether any of these correlations are statistically significant. For the period 1860-2000, with monthly data smoothed over 3-months intervals, $N \sim 500$, so the significance 95% threshold is $|\rho| \sim 0.1$. We found that correlations were significant at the 95% level everywhere in the POGA-ML ensemble mean (Fig 7, d), which very effectively isolates the response to tropical SST variability. The correlation is consistently high in this case, because of a dynamical linkage between the two basins : El Niño-induced changes in the latitudinal positions of the jets trigger changes to the transient eddy momentum fluxes in midlatitudes, which induce equatorward low-level flow at high latitudes, with a noticeable zonally-symmetric component [*Seager et al.*, 2003, 2005a]. In nature, however, this signal is potentially swamped by atmospheric dynamics independent of ENSO. Indeed, we find in the surface wind analyses (f) that the ENSO/North Atlantic connection is very weak north of $\sim 48^{\circ}N$. Repeating this analysis for five 50-year periods between 1860 and 2000 (sliding the window by 18 years each time), we found that this was due to a strong non-stationarity of the correlation in the northern parts of the basin : well above the 95% level in some decades, well below in some others. This result was also obtained for geostrophic wind fields derived from the sea-level pressure (SLP) data of *Kaplan*

et al. [2000]. This could be due either to observational error (in SST, winds, as well as SLP) or to noise. However, we found that a similar non-stationarity occurred in the GFDL simulations H1, H2 and H3, which have no measurement error. Therefore local variability is to blame in lowering the observed correlation to NINO3.

This therefore suggests the following interpretation : a link between the tropical Pacific and the North Atlantic mechanism is at work in nature as in the two GCMs, but it is of modest amplitude compared to the natural climate variability of the North Atlantic, which is quite energetic in the multidecadal spectral range. The consequence is that the link only emerges as statistically significant on long timesecales. The instrumental SLP data are consistent with this idea, albeit too short to be conclusive, and perhaps veiled by the confounding influence of anthropogenic greenhouse gas increase. The associated SLP pattern (not shown) is somewhat different than - though not completely orthogonal to - the NAO. If anything, it would resemble a more negative NAO phase, which is another way of distinguishing between this mechanism and that of *Shindell et al.* [2001] and *Hoerling et al.* [2001].

The changes shown here are of subtle magnitude, and may not be an adequate analog to millennial changes relevant to the interpretation of the IRD record. Local feedbacks must be invoked to generate a sizable response : it is possible that the ENSO-induced south-westward winds at high latitudes could cool the North Atlantic and trigger a southward ice-drift, which would also lower the local sea-surface salinity. This would weaken the buoyancy-driven circulation and its associated heat transport, further cooling the area. It is also plausible that such North Atlantic cooling would reverberate back into the Tropics [*Vellinga and Wood*, 2002; *Chi-*

ang et al., 2003; *Zhang and Delworth*, 2005], further intensifying the El Niño-like anomaly, so a positive feedback would ensue.

The important idea is that solar forcing, weak though it is, is persistent enough to seed these changes into the Tropics, from which they can be exported to high latitudes, and further amplified by feedbacks involving sea-ice and the thermohaline circulation.

5.3. Solar-induced ENSO and the Monsoons

Numerous studies have shown a significant simultaneous association between El Niño and weaker monsoon rainfall over India and southeast Asia [e.g. *Pant and Parthasarathy*, 1981; *Rasmussen and Carpenter*, 1983; *Ropelewski and Halpert*, 1987]. It is therefore natural to expect persistent anomalies of eastern Pacific SST to have a noticeable influence on the Indian and Asian Monsoons - though this could possibly involve a feedback between the two oscillations [*Chung and Nigam*, 1999].

The activity of these monsoons has been documented on a broad range of timescales, and recently been tied to abrupt climate change in the North Atlantic [*Vellinga and Wood*, 2002; *Zhang and Delworth*, 2005]. Speleothem records from northern Oman [*Neff et al.*, 2001], southern Oman [*Fleitmann et al.*, 2003], the Chinese cave of Dongge [*Wang et al.*, 2005] and anoxic sediments off the coast of Oman [*Gupta et al.*, 2003], converge to a coherent depiction of the Indian and Asian Monsoon: in all these records, there is a millennial-scale correlation of weaker monsoons with IRD deposits in the North Atlantic [*Bond et al.*, 2001]. This is consistent with periods of lower irradiance inducing an El Niño-like response.

5.4. Solar-induced ENSO and continental lake records

Two high-resolution lake records display large climate fluctuations over the Holocene, with significant correlations to solar irradiance and North Atlantic climate: Arolik Lake, in Alaska [*Hu et al.*, 2003] and lake Titicaca, in Bolivia/Peru [*Baker et al.*, 2005]. It is tempting to interpret these records in the light of our theory, since they both currently pertain to regions that are strongly affected by ENSO in modern times.

In lake Arolik , the $\delta^{18}\mathrm{O}_{\mathrm{Si}}$, $\delta\mathrm{D}_{\mathrm{Pa}}$ and BSi proxies all record coherent oscillations in phase with the IRD record of *Bond et al.* [2001] and solar indices. They are hypothesized to be controlled by local moisture convergence (precipitation minus evaporation). If one made the (plausible) assumption that these proxies are mostly determined by the annual precipitation signal, then BSi would be negatively correlated with ENSO indices [*Dai and Wigley*, 2000, Fig 1c]. Hence, periods of low solar irradiance (El Niño-like, in our theory) would display higher BSi, which would explain why they correspond to peaks in the hematite-stained grains record of the North Atlantic (section 5.2). The strong ENSO signal in wintertime temperature over coastal Alaska is likely to have have been important, though no more can be said without quantitative forward-modeling of these proxies.

In lake Titicaca, the measured $\delta^{13}\mathrm{C}$ is a proxy for lake level, also a measure of moisture convergence. Today, it lies at a nodal line of the ENSO-precipitation teleconnection pattern in northern hemisphere winter [*Seager et al.*, 2005a; *Dai and Wigley*, 2000, Fig1a and Fig1c, respectively]. Consequently we do not expect any long term stable relationship between proxies at this site and the ENSO record. However, teleconnection patterns are not immutable and it is quite likely that solar-induced variations in ENSO impacted the Lake Titicaca region but some-

times by increasing precipitation and sometimes by decreasing it. This would be recorded as a non-stationary relationship between clear millennial variability in solar proxies and ENSO on the one hand, and the lake $\delta^{13}\mathrm{C}$ on the other. If the North Atlantic responds more coherently to solar-induced ENSO variability, then we would also expect to see a non-stationary relationship between the lake record and the North Atlantic record, which appears to be the case in the Lake Titicaca record presented by *Baker et al.* [2005] (see their figure 6).

5.5. Theoretical implications of a solar-induced ENSO-like variability

Our theory implies other predictions that should be testable with existing or future data :

- **Tropical Pacific SSTs** :

Periods of increased solar irradiance should be more La Niña-like, in the absence of other radiative perturbations (e.g. volcanoes). The development of better reconstructions of solar irradiance, as well as high-resolution coral and sedimentary proxy records, will prove crucial for testing this hypothesis, during the past millennium and beyond.

- **Hemispheric Symmetry** :

Tropical SSTs can influence mid and high-latitudes via Rossby-wave teleconnections [*Hoskins and Karoly*, 1981; *Horel and Wallace*, 1981] or the transient eddy response to SST-induced strengthening of subtropical jets [*Seager et al.*, 2003, 2005a]. Both cause climate anomalies with clear hemispheric symmetry. Consequently, if solar-induced ENSO variability did actually occur, it should appear in Southern Hemisphere climate records, e.g. tree-ring records of drought-sensitive regions of South America. This is in contrast to the predictions of water-hosing experiments in the North Atlantic [*Zhang and Delworth*, 2005], which have asymmetric responses about the equator in the Pacific. It is hoped that high-resolution proxy data from the

Southern Hemisphere will soon enable us to distinguish between these competing paradigms of global climate change.

6. Discussion

6.1. Summary

We have found that solar and orbital forcing combine linearly in a way that produces ENSO variance at millennial timescales, well above the model's level of internal variability. The physics of the ocean-atmosphere system embodied in the model are able to pick out solar irradiance pertubations of intermediate amplitude ($\Delta F = 0.2\% S_o$), in the presence of a much larger orbital forcing and, remarkably, in all cases, in the presence of a realistic amount of weather noise. The low-pass filtered response, in terms of SST gradient, is quite linear : knowledge of the forcing alone enables prediction of about 72% of the variance from multivariate regression. For weak scalings of the solar irradiance ($\Delta F = 0.05\% S_o$), however, the response is indistinguishable from the variability of the unforced system.

The results confirm the importance of orbital forcing in creating conditions favorable to the growth of ENSO variance over the Holocene, and suggest that solar irradiance variability may add to millennial-scale ENSO variance.

We find qualitative agreement with high-resolution paleoclimate data and propose that ENSO mediated the response to solar irradiance discovered in the North Atlantic and monsoon records of Oman and China.

6.2. Limitations of the model arrangement

The simplicity of the model is what allows the study of the coupled system over such long timescales, yet it creates caveats that are inherent to the model's formulation, as discussed by

Clement et al. [1999]. While the chain of physical reasoning linking solar forcing to equatorial SSTs (the "thermostat" mechanism) is certainly correct as far as it goes, the climate system is complex and processes not considered in this argument might be important. Perhaps cloud feedbacks play a substantial role, although whether the feedbacks would be positive or negative is not established [*Rind*, 2002]. In a time of enhanced solar heating, the oceans should generally warm everywhere, including the subduction zones of the waters which ultimately make up the equatorial thermocline [*McCreary and Lu*, 1994]. This mechanism would complete a loop from equatorial SSTs through the atmosphere to midlatitude SSTs and then back through the ocean to equatorial SSTs. However, careful studies of Pacific SST variations in recent decades have shown that the oceanic pathway is ineffective because the midlatitude anomalies are diluted by mixing, especially as they move along the western boundary on their way to the equator [*Schneider et al.*, 1999]. Still, since subduction and advection of midlatitude waters are the ultimate source of the equatorial thermocline, this oceanic mechanism must become effective at some longer timescale, and alter the operation of the thermostat [*Hazeleger et al.*, 2001].

While the thermostat mechanism may also apply to other epochs, such as Ice Ages, the current model formulation (anomalies on top of a prescribed seasonal cycle) does not allow any such extrapolation, as the background state of the model would be quite different from what is specified here.

6.3. Forcing uncertainties

Since the SST response to the moderate forcing ($\Delta F = 0.2\% S_o$) is just at the magnitude of the drought patterns of recent times [*Seager et al.*, 2005b], any reduction in the estimate of irradiance forcing makes the Sun an implausible cause of tropical Pacific climate change,

let alone global climate change. So while there is a reasonably convincing empirical correspondence between proxies for solar output and tropical Pacific SSTs, the great uncertainties in solar irradiance forcing raise doubts about explanations of these SST variations as responses to solar forcing. Amidst such a frustrating array of uncertainties, a useful inference can still be made : for moderate to strong scalings of solar variability, it is physically plausible that ocean-atmosphere feedbacks amplify those changes above the level of internal ENSO variability, but weak scalings are unable to produce the necessary changes.

A major caveat, as stated before, is the absence of volcanic aerosol forcing in the present study. The results need to be reassessed once such a timeseries becomes available.

6.4. Conclusions

We propose that, given a mid-to-high-range amplitude of Holocene solar irradiance variations, ENSO may have acted as one of the mediators between the Sun and the Earth's climate. Air/sea feedbacks amplified solar forcing to produce persistent, El Niño-like SST anomalies at times of decreased irradiance - the thermostat mechanism. In doing so, it would have simultaneously weakened the intensity of the Indian and Asian monsoons, and triggered Bond events in the North Atlantic, generating global climate variability on centennial to millennial timescales. It is likely that other feedbacks were involved in this process, such as the wind-driven and thermohaline circulation of the ocean, and cloud feedbacks. Further research, with more complete models, will undoubtedly clarify the respective role of all these mechanisms, during interglacial and glacial periods.

So far, data from the past millennium and the longer Holocene seem to support our view. As more complete - and presumably more accurate - climate records become available, especially

from the Southern Hemisphere, we hope that our mechanism can be tested in greater detail and on longer periods.

Acknowledgments. This work was inspired by our late colleague Gerard Bond, who greatly encouraged the earlier stages of it, but passed away before he could see the completion. He influenced us more than he ever knew. We acknowledge the following grants : NOAA NA030AR4320179 P07, NOAA NA030AR4320179 20A, NSF ATM 0347009 and NSF ATM 0501878. JEG was partially supported by the Boris Bakhmeteff Fellowship in Fluid Mechanics. JEG would like to thank Gustavo Correa, Naomi Naik and Lawrence Rosen for technical assistance, and Andrew Wittenberg, Yochanan Kushnir and Steve Zebiak for many illuminating discussions.

References

Asmerom, Y., V. Polyak, J. Rasmussen, S. Burns, and M. Lachniet (2005), Persistence of ENSO-like climate variability throughout the Holocene, *Eos Trans. AGU*, *86*(52), Fall Meet. Suppl., Abstract PP53A–02.

Baker, P. A., S. C. Fritz, J. Garland, and E. Ekdahl (2005), Holocene hydrologic variation at Lake Titicaca, Bolivia/Peru, and its relationship to North Atlantic climate variation, *J. Quatern. Sc.*, *20*(7-8), 655–662.

Bard, E., G. Raisbeck, F. Yiou, and J. Jouzel (2000), Solar irradiance during the last 1200 years based on cosmogenic nuclides, *Tellus*, *52B*, 985Ð992.

Beer, J. (2000), Long-term indirect indices of solar variability, *Space Sc. Rev.*, *94*(1-2), 53–66.

Berger, A. L. (1978), Long term variations of daily insolation and Quaternary climatic changes, *J. Atmos. Sc.*, *35*(12), 2362–2367.

Bjerknes, J. (1969), Atmospheric teleconnections from the equatorial Pacific, *Mon. Weather Rev.*, *97*(3), 163.

Bond, G., et al. (2001), Persistent Solar Influence on North Atlantic Climate During the Holocene, *Science*, *294*(5549), 2130–2136.

Cane, M. A., and R. J. Patton (1984), A numerical-model for low-frequency equatorial dynamics, *J. Phys. Oceanogr.*, *14*(12), 1853–1863.

Chiang, J. C. H., M. Biasutti, and D. Battisti (2003), Sensitivity of the Atlantic ITCZ to Last Glacial Maximum boundary conditions, *Paleoceanography*, *18*(4), 1094, doi:10.1029/2003PA000916.

Chung, C., and S. Nigam (1999), Asian summer monsoon-ENSO feedback on the Cane-Zebiak model ENSO, *J. Clim.*, *12 (9)*, 2787–2807.

Clement, A. C., R. Seager, M. A. Cane, and S. E. Zebiak (1996), An ocean dynamical thermostat, *J. Clim.*, *9*(9), 2190–2196.

Clement, A. C., R. Seager, and M. A. Cane (1999), Orbital controls on the El Niño/Southern Oscillation and the tropical climate, *Paleoceanography*, *14*(4), 441–456.

Clement, A. C., R. Seager, and M. A. Cane (2000), Suppression of El Niño during the mid-Holocene by changes in the Earth's orbit, *Paleoceanography*, *15*(6), 731–737.

Cobb, K. M., C. D. Charles, H. Cheng, and R. L. Edwards (2003), El Niño/Southern Oscillation and tropical Pacific climate during the last millennium, *Nature*, *424*, 271–276.

Cook, E., C. Woodhouse, C. Eakin, D. Meko, and D. Stahle (2004), Long-term aridity changes in the western United States, *Science*, *306(5698)*, 1015–1018.

Cook, E., R. Seager, M. Cane, and D. Stahle (2006), North American drought: Reconstructions, causes, and consequences, *submitted to Earth Sc. Rev.*

Crowley, T. J. (2000), Causes of Climate Change Over the Past 1000 Years, *Science*, *289*(5477), 270–277.

Dai, A., and T. Wigley (2000), Global patterns of ENSO-induced precipitation, *Geophys. Res. Lett.*, *27*(99), 1283–1286.

Davis, M. (2001), *Late Victorian Holocausts: El Niño Famines and the Making of the Third World*, 464 pp., Verso, New York.

Eddy, J. (1977), Climate and the changing Sun, *Climatic change*, *1*(2), 173–190.

Evans, M. N., and A. Kaplan (2004), *The Pacific sector Hadley and Walker Circulations in historical marine wind analyses*, pp. 239–258, Kluwer Academic Publishers.

Fleitmann, D., S. J. Burns, M. Mudelsee, U. Neff, J. Kramers, A. Mangini, and A. Matter (2003), Holocene Forcing of the Indian Monsoon Recorded in a Stalagmite from southern Oman, *Science*, *300*(5626), 1737–1739, doi:10.1126/science.1083130.

Foukal, P., G. North, and T. Wigley (2004), A Stellar View on Solar Variations and Climate, *Science*, *306*(5693), 68–69.

Fröhlich, C., and J. Lean (2004), Solar radiative output and its variability: evidence and mechanisms, *Astron. Astrophys. Rev.*, *12*, 273–320.

Geller, M., and J. Alpert (1980), Planetary wave coupling between the troposphere and the middle atmosphere as a possible Sun-weather mechanism, *J. Atmos. Sc.*, *37*, 1197–1215.

Ghil, M., et al. (2002), Advanced spectral methods for climatic time series, *Rev. Geophys.*, *40*(1), 1003–1052.

Gill, A. E. (1980), Some simple solutions for heat-induced tropical circulations, *Quart. J. Roy. Meteor. Soc.*, *108*, 447–462.

Gupta, A., D. Anderson, and J. Overpeck (2003), Abrupt changes in the Asian southwest monsoon during the Holocene and their links to the North Atlantic Ocean, *Nature*, *421*(6921), 354–357.

Haigh, J. D. (1996), The Impact of Solar Variability on Climate, *Science*, *272*(5264), 981–984.

Hazeleger, W., R. Seager, M. Visbeck, N. H. Naik, and K. Rodgers (2001), Impact of the mid-latitude storm track on the upper pacific ocean, *J. Phys. Oceanogr.*, *31*(2), 616–636.

Herweijer, C., and R. Seager (2006), The global footprint of persistent extra-tropical drought in the instrumental era, *Int. J. of Clim.*, *submitted*.

Herweijer, C., R. Seager, and E. Cook (2006a), North American droughts of the mid-to-late nineteenth century: a history, simulation and implication for mediaeval drought, *The Holocene*, *16*.

Herweijer, C., R. Seager, E. Cook, and J. Emile-Geay (2006b), North american droughts of the last millennium from a gridded network of tree-ring data, *J. Clim.*, *submitted*.

Hoerling, M. P., J. W. Hurrell, and T. Xu (2001), Tropical origins for recent North Atlantic climate change, *Science*, *292*(5514), 90–92.

Horel, J., and J. Wallace (1981), Planetary-scale atmospheric phenomena associated with the Southern Oscillation, *Mon. Weather Rev.*, *109*, 814–829.

Hoskins, B., and D. Karoly (1981), The steady linear response of a spherical atmosphere to thermal and orographic forcing, *J. Atmos. Sci.*, *38*, 1179–1196.

Hu, F. S., et al. (2003), Cyclic variation and solar forcing of Holocene climate in the Alaskan Subarctic, *Science*, *301*(5641), 1890–1893.

Jones, P., and M. Mann (2004), Climate over past millennia, *Reviews of Geophysics*, *42*, doi: doi:10.1029/2003RG000143.

Kaplan, A., M. A. Cane, Y. Kushnir, A. C. Clement, M. B. Blumenthal, and B. Rajagopalan (1998), Analyses of global sea surface temperature 1856-1991, *J. Geophys. Res. Oceans*, *103*(C9), 18,567–18,589.

Kaplan, A., Y. Kushnir, and M. Cane (2000), Reduced space optimal interpolation of historical marine sea level pressure: 1854-1992, *J. Clim.*, *13*(16).

Karspeck, A., S. R., and M. A. Cane (2004), Predictability of tropical Pacific decadal variability in an intermediate model, *J. Clim*, *18*, 2842–2850.

Lean, J. L., Y.-M. Wang, and N. R. Sheeley (2002), The effect of increasing solar activity on the sun's total and open magnetic flux during multiple cycles: Implications for solar forcing of climate, *Geophys. Res. Lett.*, *29*, 77–1.

Mann, M. E., M. A. Cane, S. E. Zebiak, and A. Clement (2005), Volcanic and solar forcing of the tropical Pacific over the past 1000 years, *J. Clim.*, *18(3)*, 447–456.

Marchal, O. (2005), Optimal estimation of atmospheric ^{14}C production over the Holocene: paleoclimate implications, *Clim. Dyn.*, *24(1)*, 71–88.

McCreary, J. P., and P. Lu (1994), Interaction between the subtropical and equatorial ocean circulations: The subtropical cell, *J. Phys. Oceanogr.*, *24*, 466–497.

Mordvinov, A., N. Makarenko, M. Ogurtsov, and H. Jungner (2004), Reconstruction of magnetic activity of the Sun and changes in its irradiance on a millennium timescale using neurocomputing, *Solar Physics*, *224*(1), 247–253.

Moy, C., G. Seltzer, and D. Rodbell, D.T.and Anderson (2002), Variability of El Niño/Southern Oscillation activity at millennial timescales during the Holocene epoch, *Nature*, *420*(6912), 162–165.

Neff, U., S. Burns, A. Mangini, M. Mudelsee, D. Fleitmann, and A. Matter (2001), Strong coherence between solar variability and the monsoon in Oman between 9 and 6 kyr ago, *Nature*, *411*(6835), 290–293.

Pant, G. B., and B. Parthasarathy (1981), Some aspects of an association between the Southern Oscillation and Indian summer monsoon, *Arch. Meteorol. Geophys. Bioklimatol. Ser.*, *B 29*(245).

Peristykh, A. N., and P. E. Damon (2003), Persistence of the Gleissberg 88-year solar cycle over the last ˜12,000years: Evidence from cosmogenic isotopes, *J. Geophys. Res. Space Phys.*, *108*, 1–1, doi:10.1029/2002JA009390.

Rasmussen, E., and T. Carpenter (1982), Variations in tropical sea-surface temperature and surface winds associated with the Southern Oscillation/ El Niño, *Mon. Weather Rev.*, *110*, 354–384.

Rasmussen, E. M., and T. H. Carpenter (1983), The relationship between eastern equatorial Pacific sea surface temperatures and rainfall over India and Sri Lanka, *Mon. Weather Rev.*, *111*, 517.

Reed, R. (1977), On estimating insolation over the ocean, *J. Phys. Oceanogr.*, *7*, 482–485.

Rind, D. (2002), The Sun's Role in Climate Variations, *Science*, *296*(5568), 673–677.

Rind, D., D. Shindell, J. Perlwitz, J. Lerner, P. Lonergan, J. Lean, and C. McLinden (2004), The relative importance of solar and anthropogenic forcing of climate change between the Maunder Minimum and the present, *J. Clim.*, *17(5)*, 906–929.

Rogers, J. C. (1984), The association between the North Atlantic Oscillation and the Southern Oscillation in the Northern hemisphere, *Mon. Weather Rev.*, *112*(10), 1999– 2015, doi:10.1175/1520-0493(1984)112.

Ropelewski, C., and M. Halpert (1987), Global and regional scale precipitation patterns associated with the El Niño/Southern Oscillation, *Mon. Weather Rev.*, *115*, 1606–1626.

Saint-Onge, G., J. S. Stoner, and C. Hillaire-Marcel (2003), Holocene paleomagnetic records from the St. Lawrence Estuary, eastern Canada: centennial- to millennial-scale geomagnetic modulation of cosmogenic isotopes, *Earth Planet. Sc. Lett.*, *209*, 113–130.

Schneider, N., A. J. Miller, M. A. Alexander, and C. Deser (1999), Subduction of decadal North Pacific temperature anomalies: Observations and dynamics, *J. Phys. Oceanogr.*, *29*, 1056–1070.

Schubert, S. D., M. J. Suarez, P. J. Pegion, R. D. Koster, and J. T. Bacmeister (2004), On the Cause of the 1930s Dust Bowl, *Science*, *303*(5665), 1855–1859, doi:10.1126/science.1095048.

Seager, R., N. Harnik, Y. Kushnir, W. Robinson, and J. Miller (2003), Mechanisms of hemispherically symmetric climate variability, *J. Clim.*, *16*(18), 2960–2978.

Seager, R., N. Harnik, W. A. Robinson, Y. Kushnir, M. Ting, H. Huang, and J. Velez (2005a), Mechanisms of ENSO-forcing of hemispherically symmetric precipitation variability, *Quart.*

J. Royal Meteor. Soc., *131*, 1501–1527, doi: 10.1256/qj.04.n.

Seager, R., Y. Kushnir, C. Herweijer, N. Naik, and J. Velez (2005b), Modeling of tropical forcing of persistent droughts and pluvials over western North America : 1856-2000, *J. Clim.*, *18*(19), 4068–4091.

Shindell, D., D. Rind, N. Balachandran, J. Lean, and P. Lonergan (1999), Solar Cycle Variability, Ozone, and Climate, *Science*, *284*(5412), 305–308.

Shindell, D. T., G. A. Schmidt, M. E. Mann, D. Rind, and A. Waple (2001), Solar Forcing of Regional Climate Change During the Maunder Minimum, *Science*, *294*(5549), 2149–2152, doi:10.1126/science.1064363.

Stuiver, M., T. F. Braziunas, B. Becker, and K. N. (1991), Climatic, solar, oceanic, and geomagnetic influences on late-glacial and Holocene atmospheric $^{14}\mathrm{C}/^{12}\mathrm{C}$ change, *Quatern. Res.*, *35*(1), 1–24.

Stuiver, M., et al. (1998), INTCAL98 Radiocarbon Age Calibration, 24,000-0 cal BP, *Radiocarbon*, *40*(3), 1041–1084.

Thomson, D. J. (1982), Spectrum estimation and harmonic analysis, *Proc. IEEE*, *70(9)*, 1055–1096.

Torrence, C., and G. P. Compo (1998), A practical guide to wavelet analysis, *Bull. Amer. Meteor. Soc.*, *79*(1), 61–78.

Tudhope, A. W., et al. (2001), Variability in the El Niño-Southern Oscillation through a Glacial-Interglacial Cycle, *Science*, *291*, 1511–1516.

van Loon, H., and K. Labitzke (1988), Association between the 11-year solar cycle, the QBO, and the atmosphere. part ii: Surface and 700 mb in the Northern hemisphere in Winter, *J.*

Clim., *1*, 905–920.

Vautard, R., and M. Ghil (1989), Singular spectrum analysis in nonlinear dynamics, with applications to paleoclimatic time series, *Physica D*, *35*, 395–424.

Vellinga, M., and R. Wood (2002), Global climatic impacts of a collapse of the Atlantic thermohaline circulation, *Climatic Change*, *54*(3), 251 – 267.

Wagner, G., J. Beer, J. Masarik, R. Muscheler, P. Kubik, W. Mende, C. Laj, G. Raisbeck, and F. Yiou (2001), Presence of the solar De Vries cycle (~ 205 years) during the last Ice Age, *Geophys. Res. Lett.*, *28(2)*, 303Ð306.

Wang, Y., et al. (2005), The Holocene Asian Monsoon: Links to Solar Changes and North Atlantic Climate, *Science*, *308*(5723), 854–857, doi:10.1126/science.1106296.

Weber, S., T. Crowley, and van der Schrier G. (2004), Solar irradiance forcing of centennial climate variability during the Holocene, *Clim. Dyn.*, *22(5)*, 539 – 553.

Worley, S. J., S. D. Woodruff, R. W. Reynolds, S. J. Lubker, and N. Lott (2005), Icoads release 2.1 data and products, *Int. J. Climatol.*, *25*(7), 823–842, doi:10.1002/joc.1166.

Yiou, F., et al. (1997), Beryllium 10 in the Greenland Ice Core Project ice core at Summit, Greenland, *J. Geophys. Res.*, *102*, 26,783–26,794, doi:10.1029/97JC01265.

Zebiak, S. E. (1982), A simple atmospheric model of relevance for El Niño, *J. Atmos. Sc.*, *39*, 2017–2027.

Zebiak, S. E., and M. A. Cane (1987), A model El-Niño Southern Oscillation, *Mon. Weather Rev.*, *115*(10), 2262–2278.

Zhang, R., and T. L. Delworth (2005), Simulated tropical response to a substantial weakening of the Atlantic thermohaline circulation, *J. Clim.*, *18*(12), 1853–1860.

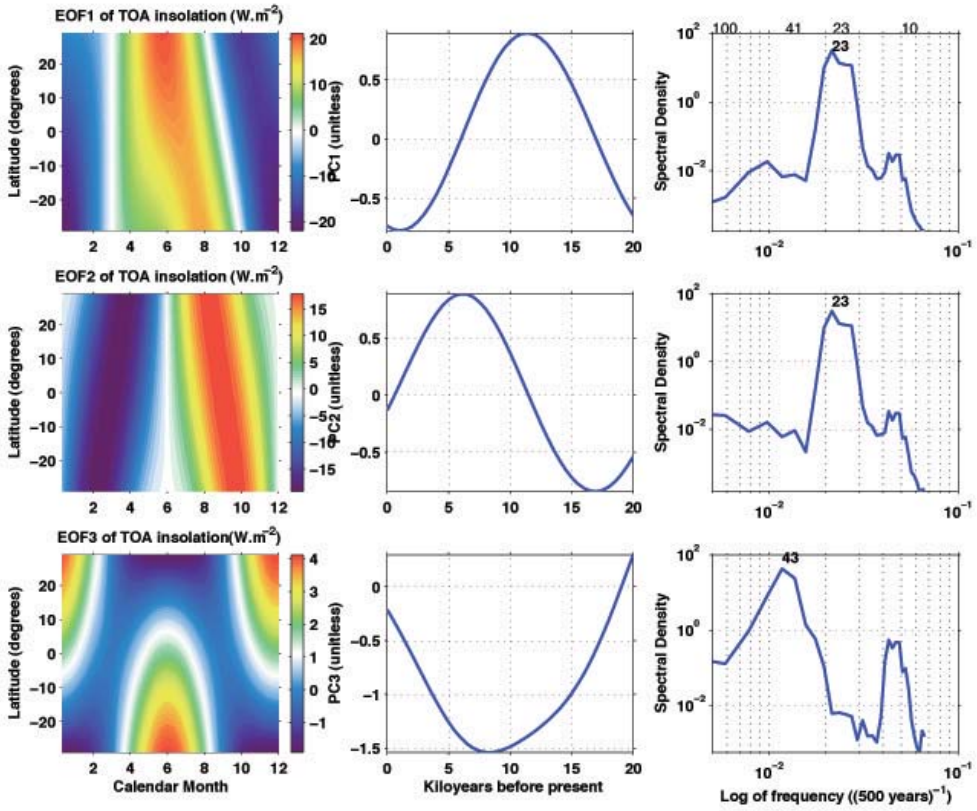

Figure 1. EOF analysis of the top-of-the-atmosphere insolation over the Holocene. The leftmost column shows the EOF pattern as a function of calendar month (Jan =1, Feb =2, etc..), the center column shows the PC timeseries, and the rightmost column its spectral density, computed with the multitaper method [*Thomson*, 1982].

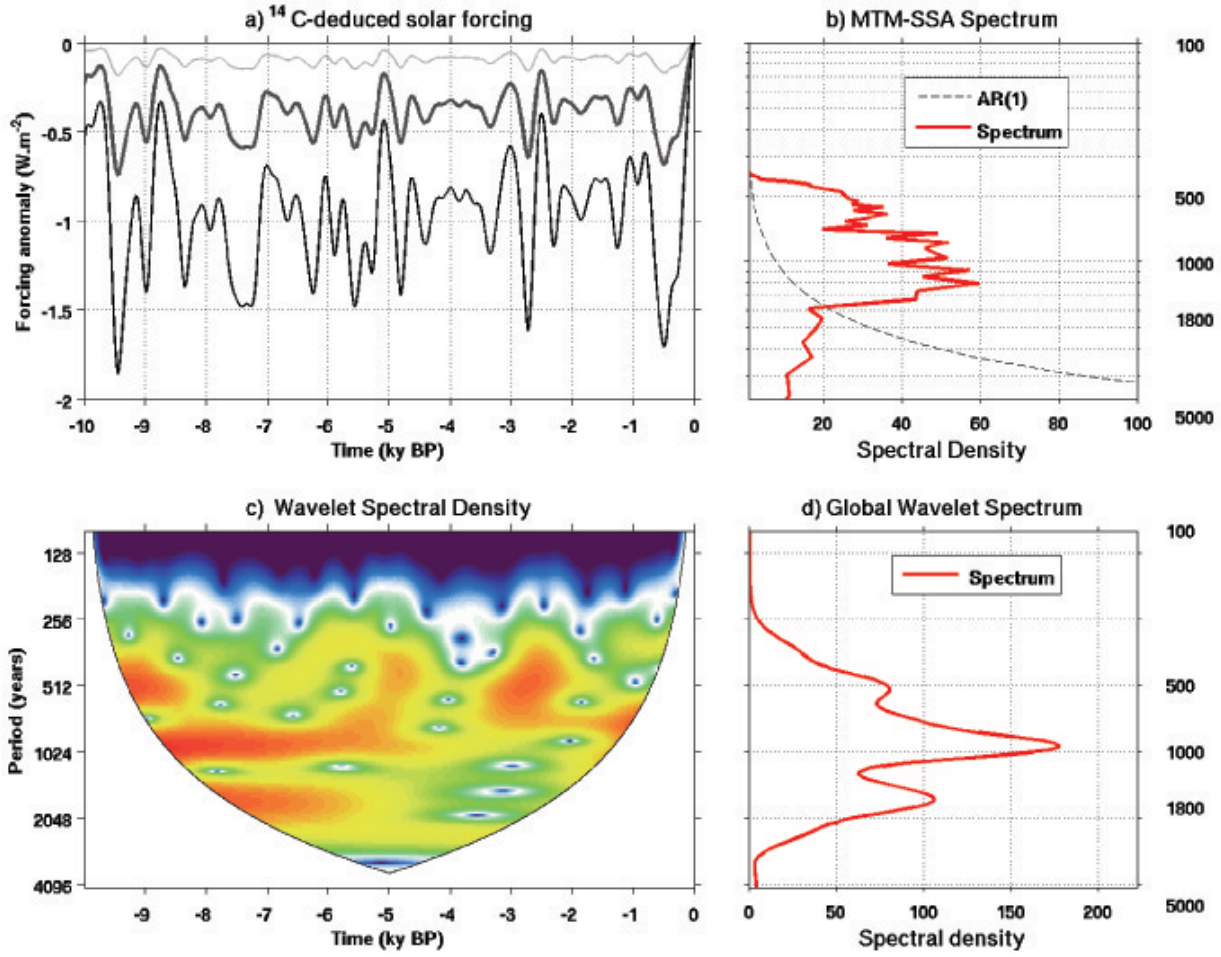

Figure 2. Spectral analysis of the ^{14}C production rate record. a) *Smoothed ^{14}C timeseries* from *Bond et al.* [2001], converted to $\mathrm{W m^{-2}}$ for 3 scalings : a Maunder Minimum solar dimming of $0.05\% \times S_o$ (light gray), $0.2\% \times S_o$ (thick, dark gray), $0.5\% \times S_o$ (thin, black) . b) *Multi-taper spectrum* after SSA pre-filtering, showing the prominence of millennial variability. c) *Wavelet spectral density*, with color scheme ranging from purple (lowest values) to red (highest). The white area is the cone-of-influence [*Torrence and Compo*, 1998] . d) *Global wavelet spectrum* , the time-average of c). The numbers right of panels b) and d) are the periodicities in years.

Table 1. Summary of the numerical experiments used in this study.

Set	Scale	Noise level	Name
Solar	0.5	40 %	Sol0.5
	0.2	40 %	Sol0.2
	0.05	40 %, 0%	Sol0.05
Orbital	- ‘	40 %, 0%	Orb
Orbital & Solar	0.5	40%	Orb_Sol_0.5
	0.2	40%	Orb_Sol_0.2

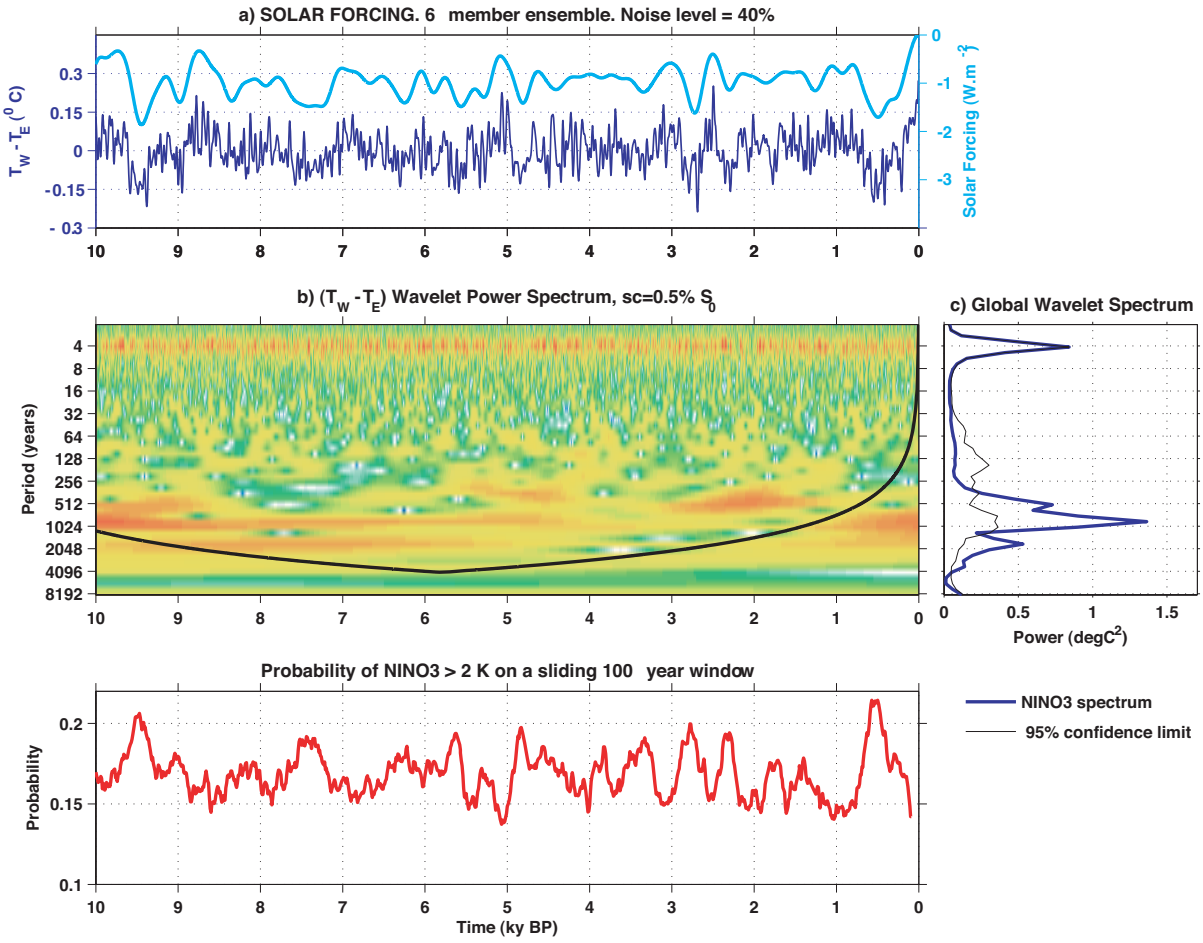

Figure 3. Model response to solar forcing ($\Delta F = 0.2\% S_o$, experiment Sol0.2). a) Solar forcing (light blue) and response ($T_W - T_E$) (dark blue). b) Wavelet spectral density (arbitrary units, with maxima in red, minima in light blue.). The thick black line is the cone-of-influence, the region under which boundary effects can no longer be ignored [*Torrence and Compo*, 1998] c) Global Wavelet Spectrum and 95 % confidence level (see text for details). d) Probability of a large El Niño event over a 200 year window.

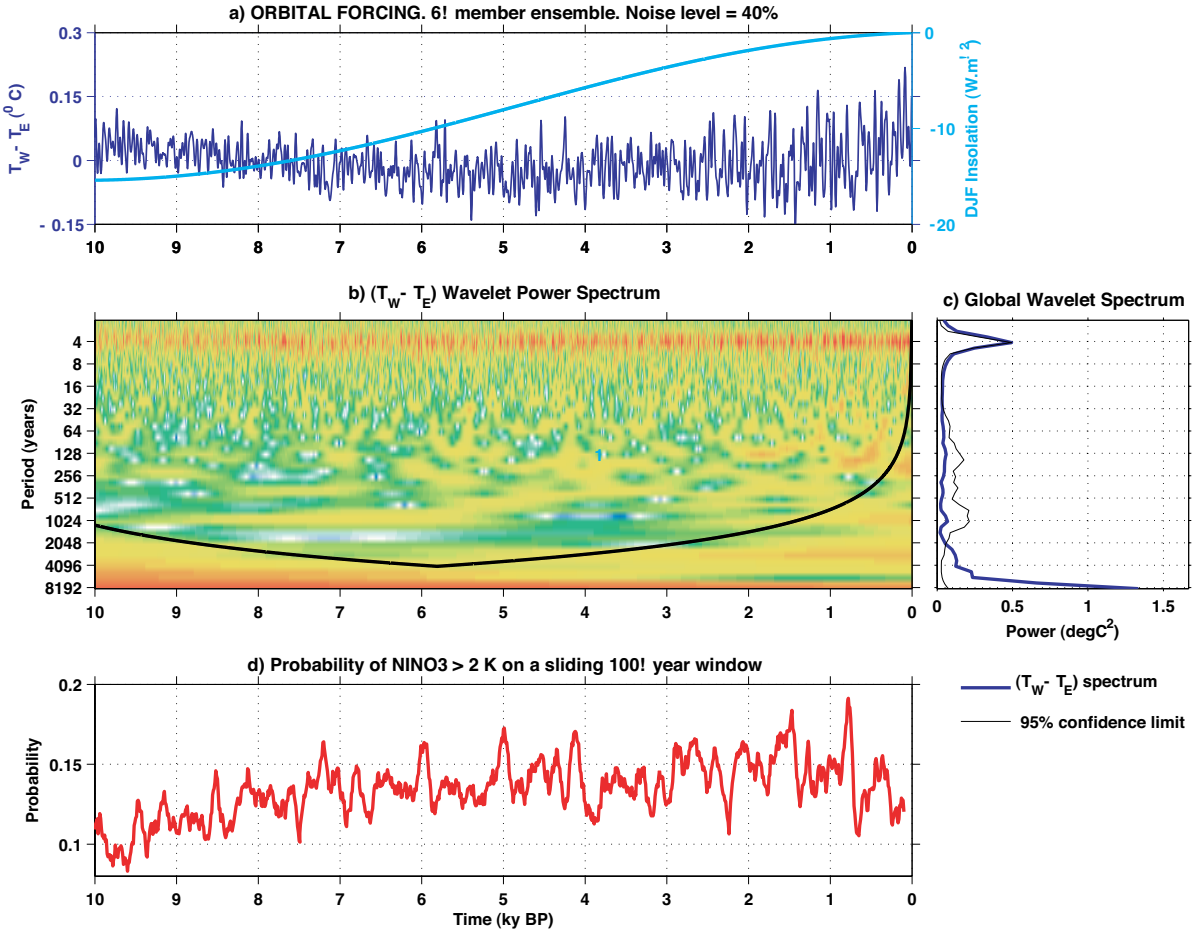

Figure 4. Same as Fig 3 but for orbital forcing (experiment Orb).

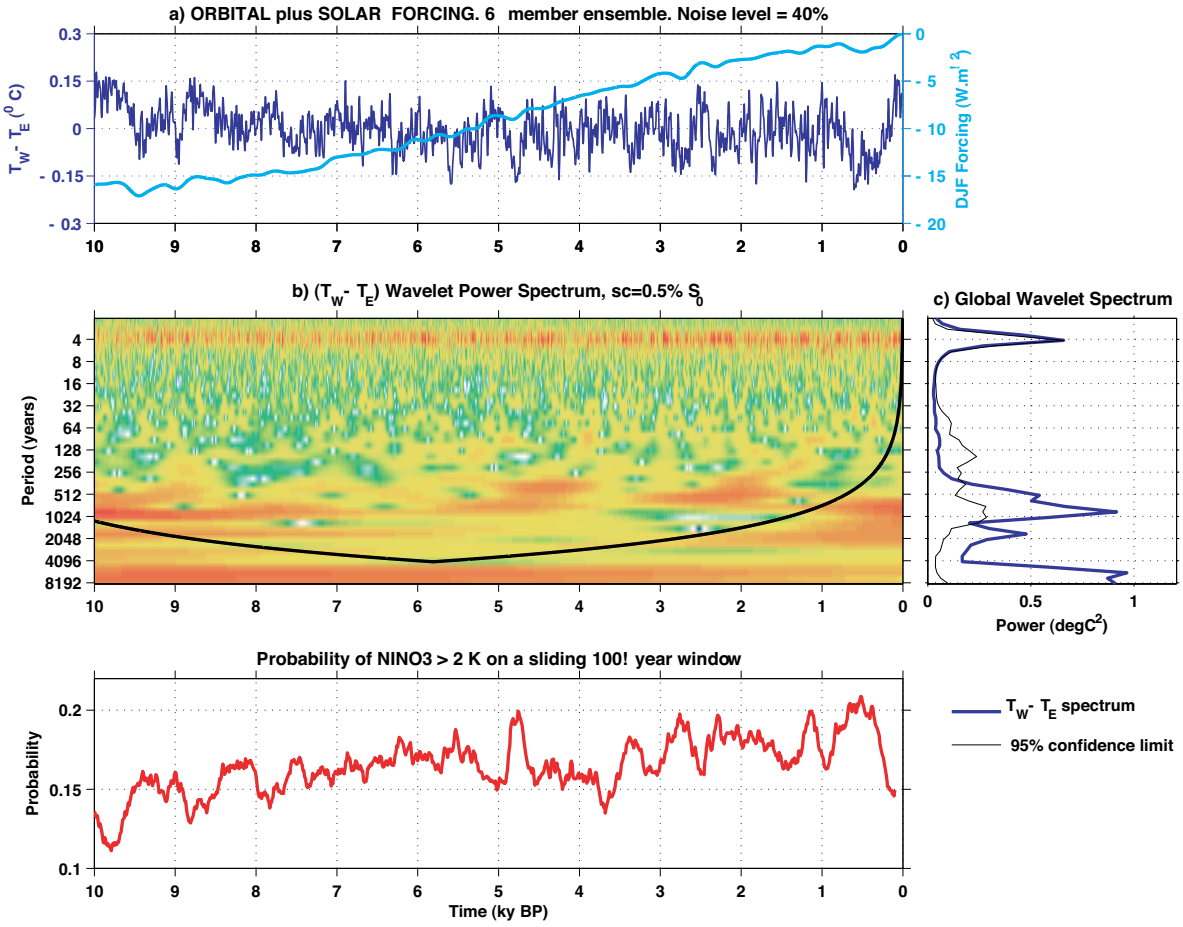

Figure 5. Same as Fig 3 but with orbital and solar forcing ($\Delta F = 0.5\% S_o$, experiment Orb_Sol_0.5).

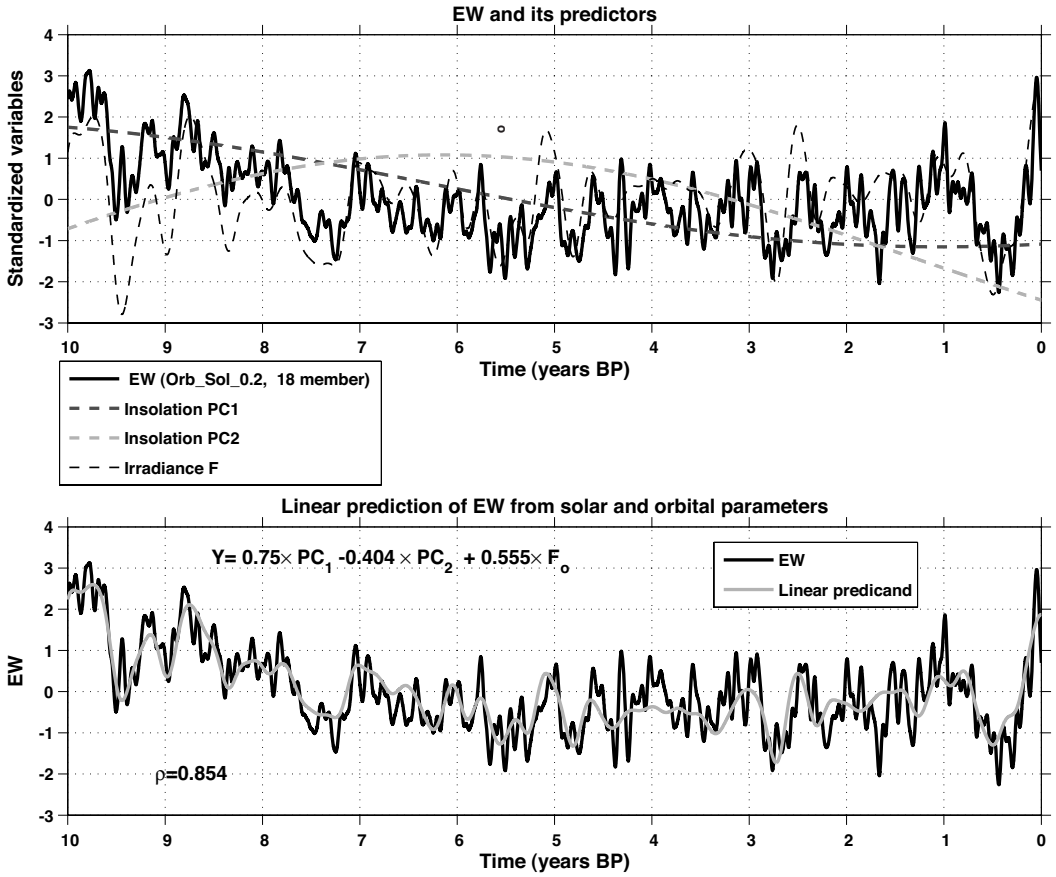

Figure 6. Linear prediction of ENSO variability from solar parameters. a) Lowpass-filtered zonal SST difference (EW), and predictor variables : PC_1 and PC_2 from Fig 1 and F_o from Fig 2, with $\Delta F = 0.2\% S_o$ b) Comparison between predicand and predicted variable. All variables were standardized prior to analysis. See text for details.

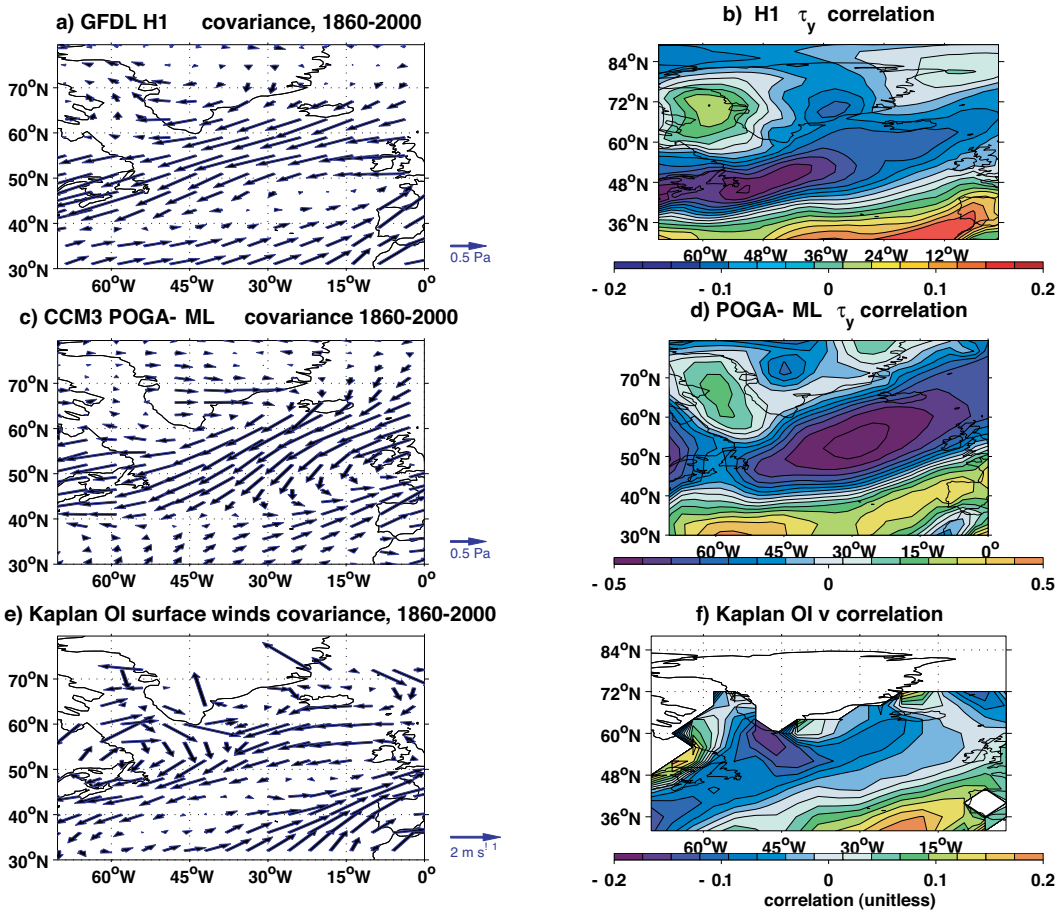

Figure 7. ENSO influence over the North Atlantic. On the left are regression patterns of wind vectors from the specified product, smoothed by a 3-month running average, on the NINO3 index, normalized to unit variance. Hence, units of regression coefficients are given per standard deviation of the index. On the right are corresponding correlation patterns, shown for the meridional component only. (a) GFDL H1 surface wind-stress regression, (b) GFDL H1 meridional wind-stress correlation. (c) POGA-ML surface wind-stress regression (d) POGA-ML meridional wind-stress correlation (e) Analysis of ICOADS data, surface wind regression (f) Analysis of ICOADS data, meridional wind correlation.